International Journal of Power Electronics and Drive System (IJPEDS)
Vol. 8, No. 4, December 2017, pp. 1455~1466
ISSN: 2088-8694, DOI: 10.11591/ijpeds.v8i4.pp1455-1466

Reactive Power Compensation in Industrial Grid via High-power Adjustable Speed Drives with Medium Voltage 3L-NPC BTB Converters

Radionov A.A., Gasiyarov V.R., Maklakov A.S., Maklakova E.A.
South Ural State University, Chelyabinsk, Russia

Article Info

Article history:

Received Sep 10, 2017
Revised Nov 18, 2017
Accepted Dec 1, 2017

Keyword:

AC-DC power converters
DC-AC power converters
Medium voltage
Reactive power control
Variable speed drives

ABSTRACT

The objective of this study is to develop and research a new method of reactive power compensation in industrial grid via high-power adjustable speed drives (HP ASDs) with medium voltage (MV) three level neutral point clamped back-to-back (3L-NPC BtB) converters. The article is concerned with the mathematical description, control system designing and obtaining of experimental results. An important advantage of the new method is that specialized equipment is not necessary for its implementation. The analysis of our experimental research shows that the developed reactive power compensation method has been successfully applied for main HP ASD of plate mill rolling state 5000 (Magnitogorsk Iron and Steel Works, PJSC). Some ways for future industrial application prospects and improvements of the designed method are outlined in the conclusion of the paper.

Corresponding Author:

Alexander S. Maklakov,
Department of Mechatronics and Automation,
South Ural State University,
76 Lenin Pr. 454080, Chelyabinsk, Russia.
Email: alexandr.maklakov.ru@ieee.org

1. INTRODUCTION

In recent years, the use of power converters has been increasing, mainly due to the global demand for electrical energy. Modern power converter topologies for high-power application are able to transmit and convert electric power with small losses and minimal negative influence on the environment [1-5]. Current economic forecast demonstrates that the converter market for power energy and industry applications will continue developing and improving in the XXIst century. «MarketsandMarkets" reports that in the years coming the volume of average annual investments in the field of power engineering will increase up to 10% [6]. Primarily, it will be connected with the renovation of energy infrastructure and implementation of renewable energy projects of Europe and the USA and with the increase of demand from fast developing economics of China, Russia, India, Brazil and South Africa [7]. Consequently, research in the field of power converters to improve energy efficiency and power quality acquire special significance [8-10].

Currently, non-reversible and reversible medium voltage (MV) high-power (HP) adjustable speed drives (ASDs) based on multilevel converter topologies are main electrical energy consumers in oil, gas, metallurgical, mining, chemical, cement, paper and other industry applications [11-13].

HP ASDs can be found commercially in single or paralleled units ranging from a power capacity of 0.4 to 200 MVA. They operate at the medium-voltage of 2.3 to 13.8 kV, however, a typical drive voltage is 3.3 kV. The operation of HP ASDs in MV has some benefits such as lower current ratings, smaller cables, smaller dc-link energy storage components and higher efficiency; therefore, it is the mainstream solution found in the HP-ASDs in practice [14].

MV 3L-NPC BtB converters are most often applied for the HP ASDs in industrial enterprises. Typical power circuits as an illustration are shown in Figure 1. Because of the toughening of international standards to electromagnetic compatibility (EMC) and power quality, multipulse grid connection circuits are the most promising for both raising energy efficiency and the quality of converted energy. These circuits are used at one of the world's largest steel producers and a leading Russian metals company Magnitogorsk Iron and Steel Works, PJSC.

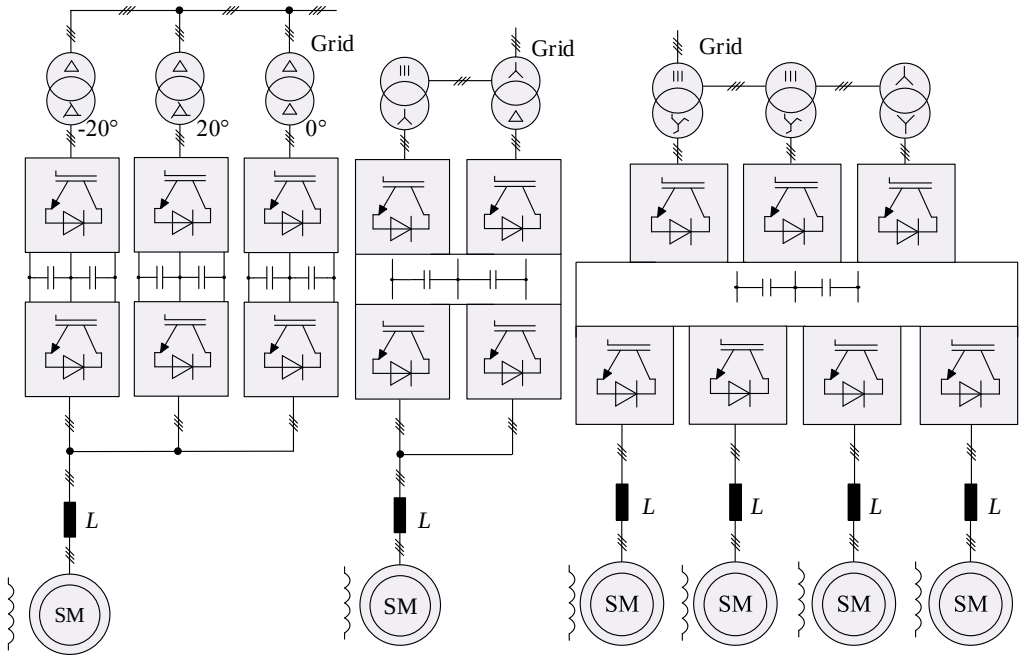

Figure 1. Power circuits for HP ASDs: a) 5000 mm plate mill, b) 1750 mm hot-strip mill and 2000 mm cold mill, c) 2000 mm cold mill (MMK Atakas)

2. PROBLEM DEFINITION AND ARTICLE PURPOSES

Currently, power quality and energy efficiency are the most important direction in the enterprise development to reduce production costs. In practice, our experience indicates that distribution grid companies penalize industrial plants for high level of consumed reactive power. In such situation, it is profitable to provide an industrial distribution grid with proper reactive power control. Furthermore, the profound effects reactive power has on the security, efficiency and transmission capacity of industrial grid are well-known [15-17].

Reactive power compensation is one of the most effective ways to reduce consumed electric energy and improve power quality. The examples of how reactive power compensation can improve the technical-and-economic indexes of an industrial power grid are [18-21]:

a. Reduce cost and generate higher revenue for the customer;
b. Reduce network losses;
c. Avoid penalty charges from utilities for excessive consumption of reactive power;
d. Increase system capacity and save costs on new installations;
e. Improve system power factor;
f. Increase power availability;
g. Improve voltage regulation in the network.

Nowadays, static VAR compensators (SVCs) and static synchronous compensators (STATCOMs) are the most useful to control the dynamic reactive power level in the industrial grid [22-24]. It is important to note the main difference between STATCOM and 3L-NPC BtB converters is their load sides, but there is the same connection in the grid side.

The majority of cases reported in the literature relate to the static reactive power compensation using active front-end (AFE) rectifier. This approach was firstly introduced for the dragline eclectic drives

case in [25]. In addition, most existing works in this field have been done using either wind or solar electrical systems [26].

This article will present some experiments showing the potential use of dynamic reactive power compensation via HP ASDs with medium voltage 3L-NPC BtB converters. A new method of the reactive power control that has been applied for this problem is described. As a research object, the main HP ASDs of the plate mill rolling state 5000 (Magnitogorsk Iron and Steel Works, PJSC) has been chosen. To investigate a reactive power compensation mode, it is necessary to perform synthesis of the new control system of the 3L-NPC BtB converter for operating conditions of the main HP ASDs of the plate mill rolling state 5000 by using a mathematical description.

3. 3L-BTB-NPC CONVERTER AS CONTROLLING OBJECT

The well-known mathematical models of multilevel converters are based on a splitting method. It allows one to split electrical circuit on sub-electrical circuits and to ensure their interaction. However, such a way does not provide for the making of convenient mathematical models and development of a control system [27-29].

The 3L-BtB-NPC converter as shown in Figure 1 contains 24 semiconductor power modules VT_1-VT_{24}, 24 forward diodes VD_1-VD_{24}, 12 clamped diodes VD_{c1}-VD_{c12} and two equivalent capacitors C_{dc1}-C_{dc2} between which a neutral point 0 is formed [14-16]. The mathematical description method is based on discrete logic functions γ_{abc}, -semiconductor device switching states $S_{abc12rv}$ for the 3L-BtB-NPC converter (grid and load side)

$$\gamma_{abcrv}=\begin{cases}1,\ \left(S_{abc1rv}\ and\ S_{abc2rv}\right)=1\ and\ \left(S_{abc3rv}\ and\ S_{abc4rv}\right)=0\\ 0,\ \left(S_{abc2rv}\ and\ S_{abc3rv}\right)=1\ and\ \left(S_{abc1rv}\ or\ S_{abc4rv}\right)=0\\ -1,\left(S_{abc3rv}\ and\ S_{abc4rv}\right)=1\ and\ \left(S_{abc1rv}\ and\ S_{abc2rv}\right)=0\end{cases} \quad (1)$$

-load side

$$\gamma_{abcv}=\begin{cases}1,\ \left(S_{abc1v}\ and\ S_{abc2v}\right)=1\ and\ \left(S_{abc3v}\ and\ S_{abc4v}\right)=0\\ 0,\ \left(S_{abc2v}\ and\ S_{abc3v}\right)=1\ and\ \left(S_{abc1v}\ or\ S_{abc4v}\right)=0\\ -1,\left(S_{abc3v}\ and\ S_{abc4v}\right)=1\ and\ \left(S_{abc1v}\ and\ S_{abc2v}\right)=0\end{cases} \quad (2)$$

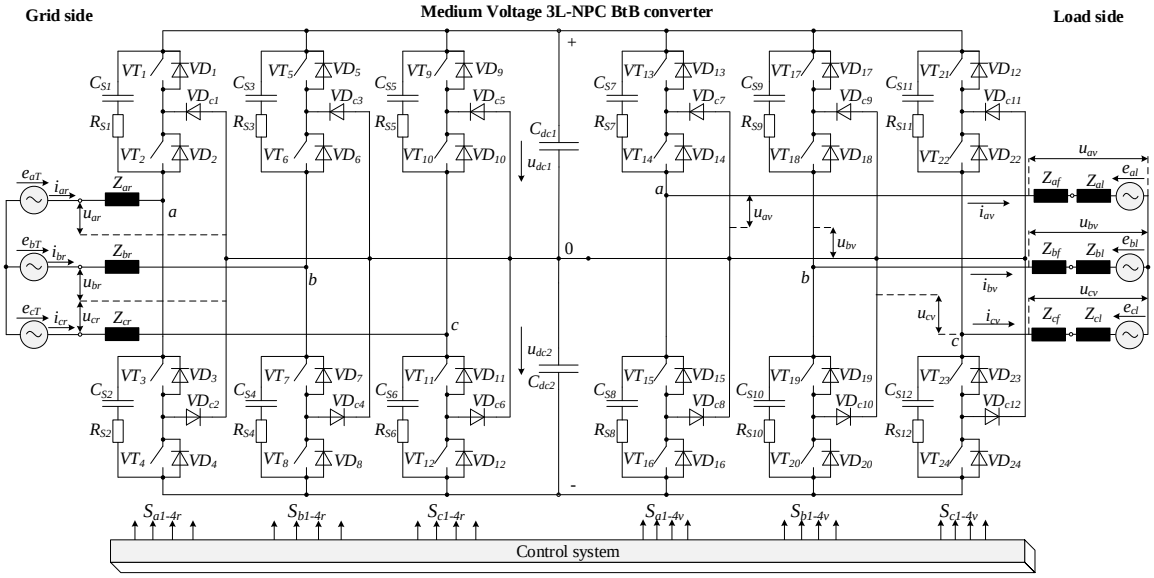

Figure 2. Power circuit of 3L-NPC BtB converter

The discrete logic functions γ_{abc} form the states of the switching functions $F_{abc12rv}$. The switching functions $F_{abc12rv}$ form the logical signals that determine the level of the DC link voltage for each phase of the 3L-BtB-NPC converter

$$F_{abc12rv} = \frac{\gamma_{abcrv} \cdot \left(\gamma_{abcrv} \pm 1\right)}{2} \tag{3}$$

According to Kirchhoff's laws, system equation was derived as

$$\begin{cases} u_{abcT} = u_{abcr} + i_{abcr} Z_{abcr} \\ u_{abcl} = u_{abcv} + i_{abcv} \left(Z_{abcf} + Z_{abcl}\right) \\ u_{abcr} = u_{dc1} \left(F_{abc1r} - \frac{1}{3}\sum_{n=a}^{b.c} F_{n1r}\right) + u_{dc2} \left(F_{abc2r} - \frac{1}{3}\sum_{n=a}^{b.c} F_{n2r}\right) \\ u_{abcv} = u_{dc1} \left(F_{abc1v} - \frac{1}{3}\sum_{n=a}^{b.c} F_{n1v}\right) + u_{dc2} \left(F_{abc2v} - \frac{1}{3}\sum_{n=a}^{b.c} F_{n2v}\right) \\ u_{dc1} = \frac{\left(F_{a1r} i_{ar} + F_{b1r} i_{br} + F_{c1r} i_{cr}\right) - \left(F_{a1v} i_{av} + F_{b1v} i_{bv} + F_{c1v} i_{cv}\right)}{p \cdot C_{dc1}} \\ u_{dc2} = \frac{\left(F_{a2r} i_{ar} + F_{b2r} i_{br} + F_{c2r} i_{cr}\right) - \left(F_{a2v} i_{av} + F_{b2v} i_{bv} + F_{c2v} i_{cv}\right)}{p \cdot C_{dc2}} \\ P_r = u_{aT} \cdot i_{ar} + u_{bT} \cdot i_{br} + u_{cT} \cdot i_{cr} \\ Q_r = \frac{1}{\sqrt{3}} \left(u_{abT} \cdot i_{cr} + u_{bcT} \cdot i_{ar} + u_{caT} \cdot i_{br}\right) \end{cases} \tag{4}$$

where i_{abcr} and i_{abcv} – grid and load side phase currents, A; Z_{abcr} and Z_{abcv} – grid and load side complex impedance, Ohm; u_{abcT} and u_{abcl} – grid and load side phase voltages, V; u_{abcr} and u_{abcv} – grid and load side 3L-NPC BtB converter voltages, V; u_{dc12} – DC voltages, V; P_r and Q_r – grid side active and reactive power, W, VAR; p – operator of differentiation.

Then, the system Equation (4) was transformed into a rotating coordinate system dq using the Park transformation. The voltage grid orientation for the grid side and load voltage orientation for the load side were used. After applying the transformation, the system (4) has the following view

$$\begin{cases} u_{dT} = u_{dr} + i_{dr} \cdot Z_{dr} - \omega_T \cdot Z_{qr} \cdot i_{qr} \\ u_{qT} = u_{qr} + i_{qr} \cdot Z_{qr} + \omega_T \cdot Z_{dr} \cdot i_{dr} \\ u_{dl} = u_{dv} + i_{dv} \cdot \left(Z_{df} + Z_{dl}\right) - \omega_l \cdot \left(Z_{qf} + Z_{ql}\right) \cdot i_{qv} \\ u_{ql} = u_{qv} + i_{qv} \cdot \left(Z_{qf} + Z_{ql}\right) + \omega_l \cdot \left(Z_{df} + Z_{dl}\right) \cdot i_{dv} \\ u_{dqr} = u_{dc1} \cdot F_{dq1r} + u_{dc2} \cdot F_{dq2r} \\ u_{dqv} = u_{dc1} \cdot F_{dq1v} + u_{dc2} \cdot F_{dq2v} \\ u_{dc1} = \frac{3}{2} \cdot \frac{\left(F_{d1r} \cdot i_{dr} + F_{q1r} \cdot i_{qr}\right) - \left(F_{d1v} \cdot i_{dv} + F_{q1v} \cdot i_{qv}\right)}{C_{dc1} \cdot p} \\ u_{dc2} = \frac{3}{2} \cdot \frac{\left(F_{d2r} \cdot i_{dr} + F_{q2r} \cdot i_{qr}\right) - \left(F_{d2v} \cdot i_{dv} + F_{q2v} \cdot i_{qv}\right)}{C_{dc2} \cdot p} \\ P_r = u_{dT} \cdot i_{dr} + u_{qT} \cdot i_{qr} \\ Q_r = -u_{qT} \cdot i_{dr} + u_{dT} \cdot i_{qr} \end{cases} \tag{5}$$

where i_{dqr} and i_{dqv} – grid and load side *dq* phase currents, A; Z_{dqr} and Z_{dqv} – grid and load side *dq* complex impedance, Ohm; u_{dqT} and u_{dql} – grid and load side *dq* phase voltages, V; u_{dqr} and u_{dqv} – grid and load *dq* side 3L-NPC BtB converter voltages, V; $F_{abc12rv}$ – *dq* switching functions; ω_t and ω_l – grid and load side *dq* angular frequencies. In our case, for the system (5) active i_d and reactive i_q currents of the 3L-BtB-NPC converter are regulated by the VOC which functional diagram is shown in Figure 3.

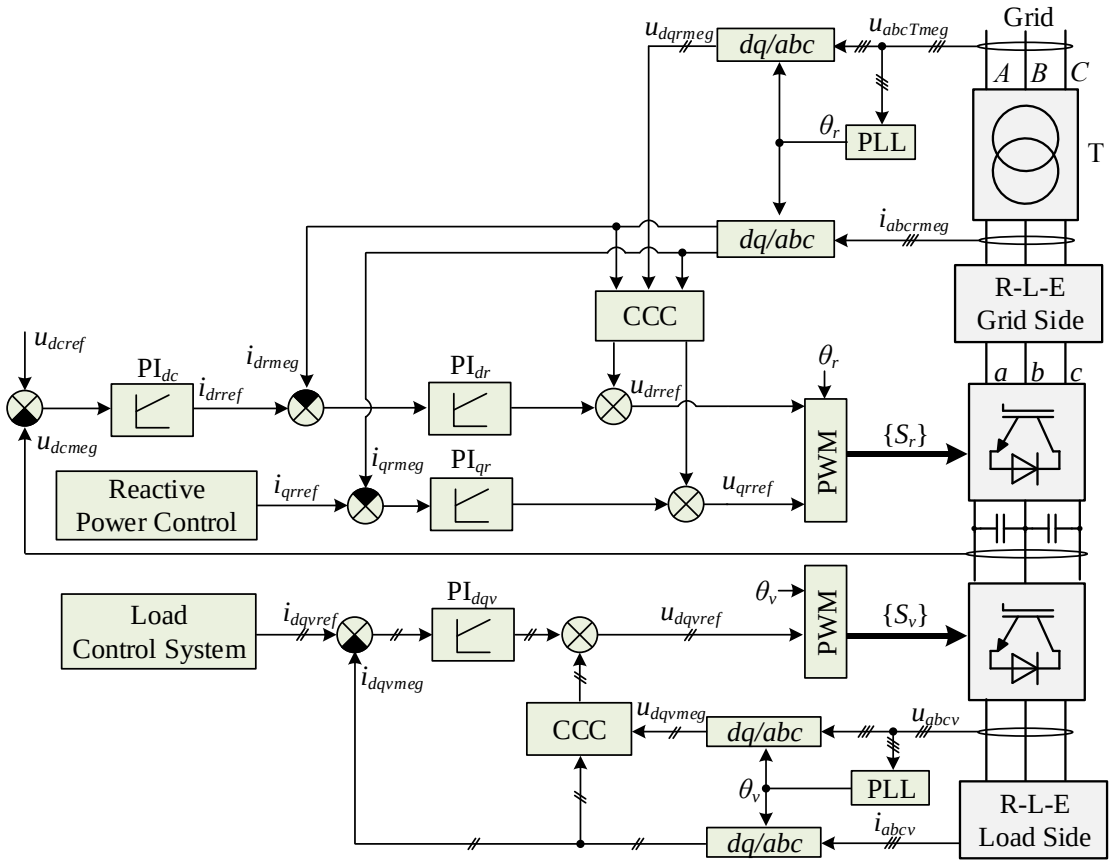

Figure 3. Functional diagram of the control system

The control system is two-loop and consists of two-channel current control systems and the external DC voltage control loop, reactive power control loop and a load control system. It allows for a separate regulating of the active i_d and reactive i_q current components. To realize this linear control method, the *abc/dq* transformation for the measured phase current i_{abcmeg} to i_{dqmeg} has been applied. Deviations from the difference between the reference current signals i_{dqref} and measured current signals i_{dqmeg} are processed by PI current controllers. Additional signals from cross-coupling compensation (CCC) blocks are the summed outputs of PI current controllers and fed to the PWM units. Phase-locked loops (PLLs) are used to calculate grid and load voltage angles θ_{rv}. The active current loop of the grid side is subordinated to the external DC voltage control loop. Deviations from the difference between the reference DC voltage signal u_{dcref} and measured DC voltage signals u_{dcmeg} are processed by a DC voltage controller. The internal reactive current loop i_{qr} is subordinated to the external reactive power control system.

Control system designing with a reactive control loop was synthesized on the basis of the system "3L-NPC BtB converter – industrial grid" shown in Figure 4. This system consists of voltage E_{BtB}, equivalent inductance L_2, equivalent resistance R_2, transformer T, grid voltage E_g, transformer secondary winding voltage E_T, equivalent inductance L_1, and equivalent resistance R_1.

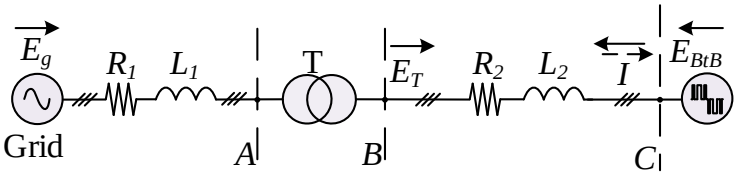

Figure 4. System "3L-NPC BtB converter – industrial grid"

The power flow from the point *B* to the point *C* can be calculated based on the following Equations [23-27]

$$P_{BC} = \frac{E_T \cdot E_{\mathrm{BtB}} \cdot \left(R_2 \cdot \cos(\alpha) + X_2 \cdot \sin(\alpha)\right) - {E_T}^2 \cdot R_2}{{R_2}^2 + {X_2}^2} \tag{6}$$

$$Q_{BC} = \frac{E_T \cdot E_{BtB} \cdot \left(X_2 \cdot \cos(\alpha) - R_2 \cdot \sin(\alpha)\right) - {E_T}^2 \cdot X_2}{{R_2}^2 + {X_2}^2} \tag{7}$$

$$S_{BC} = \sqrt{\frac{{E_T}^2 \cdot \left({E_{BtB}}^2 - 2 \cdot E_{BtB} \cdot E_T \cdot \cos(\alpha) + {E_T}^2\right)}{{R_2}^2 + {X_2}^2}} \tag{8}$$

where $P_{BC} = f(E_{BtB}, \alpha)$, $Q_{BC} = f(E_{BtB}, \alpha)$, $S_{BC} = f(E_{BtB}, \alpha)$ - active, reactive and apparent power functions in the system "3L-NPC BtB converter- industrial grid"; E_T - secondary voltage transformer; α-shift angle between E_T and E_{BtB}. The apparent power function $S_{BC} = f(E_{BtB}, \alpha)$ has been applied to reactive power control by the shift angle α and the voltage E_{BtB}. As shown in Figure 5.

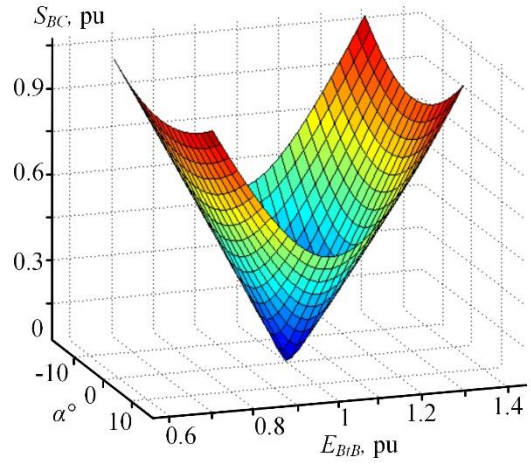

Figure 5. Apparent power function in the system "3L-NPC BtB converter – industrial grid"

A limitation level of supplying reactive power Q_{BClim} is calculated offline for each reference DC voltage by the following Equation

$$Q_{BC\,\mathrm{lim}} = \sqrt{{S_{BC}}^2 - {P_{BC}}^2} \tag{9}$$

The Equations (6-9) were used to define maximum apparent and reactive power in the connection point of the industrial grid and the ASDs with the 3L-NPC BtB converters. Using calculated results, it allowed compensating a share of the static or dynamic excess reactive power in the grid via the ASDs. It is

noted that a range of the shift angle between the transformer secondary winding voltage and the 3L-NPC BtB voltage is low. It indicates that the reactive power control system have to provide high accuracy and performance reliability in all operation conditions of the ASDs with the 3L-NPC BtB converters [30-32].

A functional scheme of the proposed reactive power control method is shown in Figure 6. The scheme provides a real-time measurement of the reactive power at the secondary control level and produce a reactive power reference signal at the local control level of the 3L-NPC BtB converter. If in the connection point of substation and the ASDs there is a requirement to increase or reduce the reactive power level, the 3L-NPC BTB converters will be able to generate or consume a shape of reference reactive power. An important advantage of the new method is that specialized equipment is not necessary for the implementation.

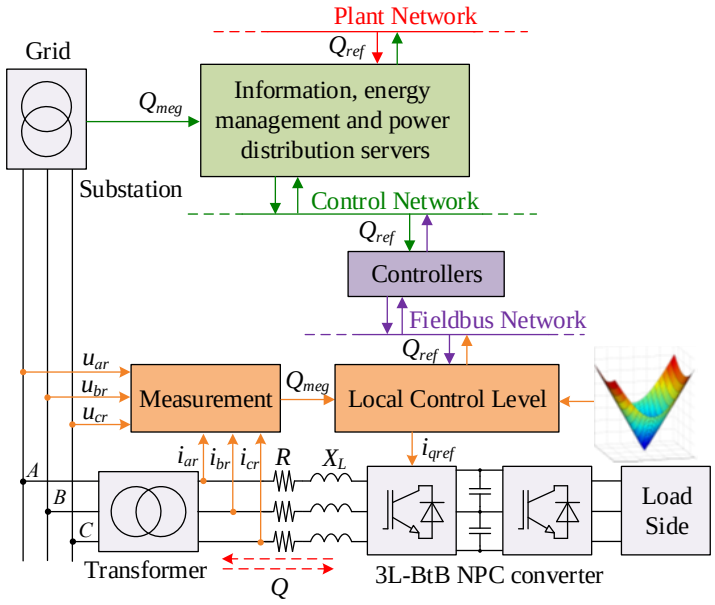

Figure 6. Functional diagram of the reactive power control system

4. RESEARCH OBJECT

The main HP ASDs of the plate mill rolling state 5000 (Magnitogorsk Iron and Steel Works, PJSC) was used as a study object. The drive comprises two synchronous motors (SMs) for each work roll, six 3L-NPC BtB converters, 18-pulse connection based converters on three power transformers with the voltages phase shifts 20°, 0°, and -20° of the secondary windings. Basic technical information of the SMs, 3L-NPC BtB converters and the power transformers is presented in Table 1. The 3L-NPC BtB converters of the considered HP ASDs are able to convert 30 MVA instantaneous peak apparent power. It is a maximum power Smax ≈ Pmax at the unit power factor. Furthermore, the 3L-NPC BtB converters can provide the power factor ±0.8, i.e. generate or consume about 20 MVAR reactive power.

Table 1. SM Technical Information

P_{rat}, [MW]	U_{rat}, [V]	I_{rat}, [A]	f_{rat}, [Hz]	cos(φ)
12	3300	2460	10	1
3L-NPC BTB Converter Technical Information				
P_{rat}, [MW]	U_{rat}, [V]	I_{rat}, [A]	f_{sw}, [Hz]	U_{dcrat}, [V]
8.4	3300	800	500	5020
Power Transformer Technical Information				
S_{rat}, [MVA]	U_1, [kV]	U_2, [kV]	I_1, [A]	I_2, [A]	U_{sc}, [%]
3300	10	3.3	329	997	16

Figure 7 shows the developed reactive power control system for the main HP ASDs of the plate mill rolling state 5000 (Magnitogorsk Iron and Steel Works, PJSC). The industrial grid is based on Smart Grid technology in which the HP ASDs with the 3L-NPC BtB converters operate in parallel with the nonlinear and reactive load. The load can be the not ASDs or ASDs with unidirectional and bidirectional AC-DC converters using diode or thyristor rectifiers.

5. RESEARCH RESULTS

Transition processes were obtained by using the ibaAnalyzer software at the sample frequency 500 Hz. The operation conditions of the main HP ASD of the plate mill rolling state 5000 in the range of roughing and finishing rolling for the difficult-to-form steel grade are shown in Figure 8 and Figure 9. These experiments were carried out without reactive power consuming and generating. The following nomenclature was taken: w_m – SM angular speed, s^{-1}; M_m – SM torque, MNm; P_g, S_g – consumed active and apparent power in the grid connection, MW and MVA; t – time, s.

Figure 9 shows that the main HP ASD of the plate mill rolling state 5000 has a maximum load at finish rolling and there is no possibility to generate additional reactive power. But in Figure 8 it is clearly seen that at roughing there is an underutilization of the apparent power.

Based on the experimental results, it was concluded that the main HP ASD of the plate mill rolling state 5000 can be applied as a static or dynamic reactive power compensator in the range of roughing. Using the designed reactive power control (Chapter III. B), it was possible to achieve 6.4 MVAR reactive power generation in all the roughing range of the main HP ASD of the plate mill rolling state 5000 (Magnitogorsk Iron and Steel Works, PJSC). It is clearly seen in Figure 10.

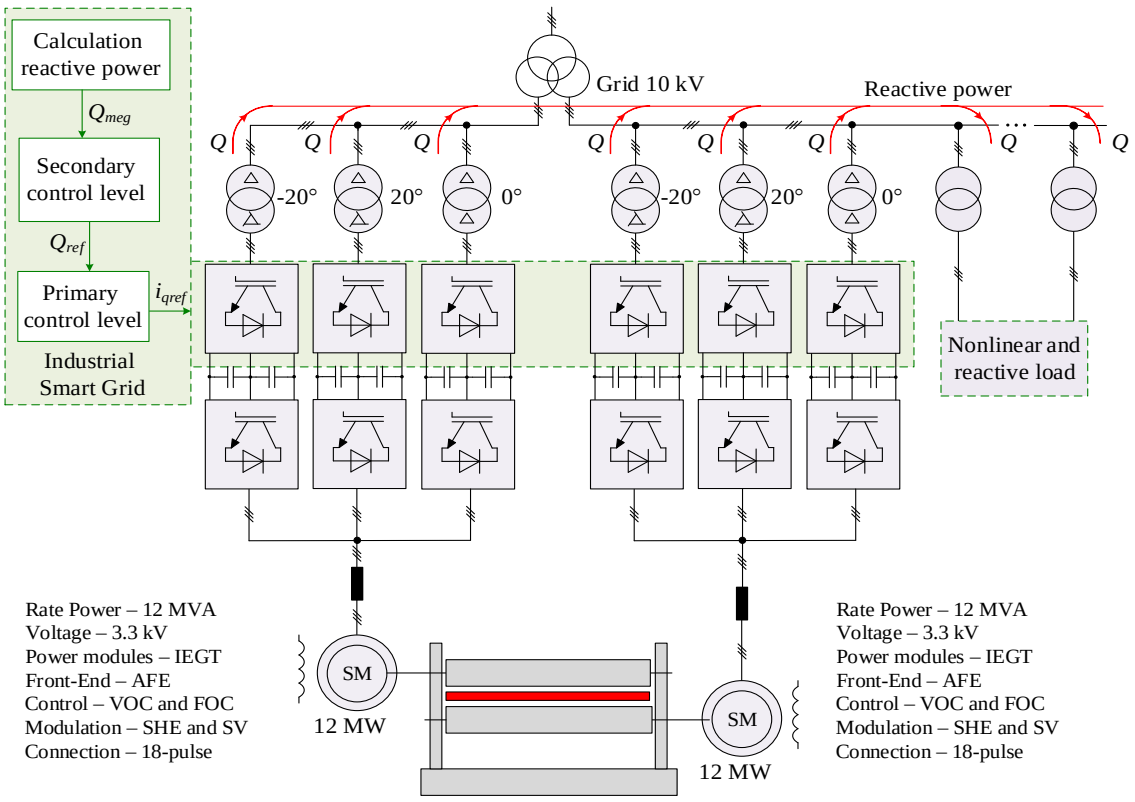

Figure 7. Research object

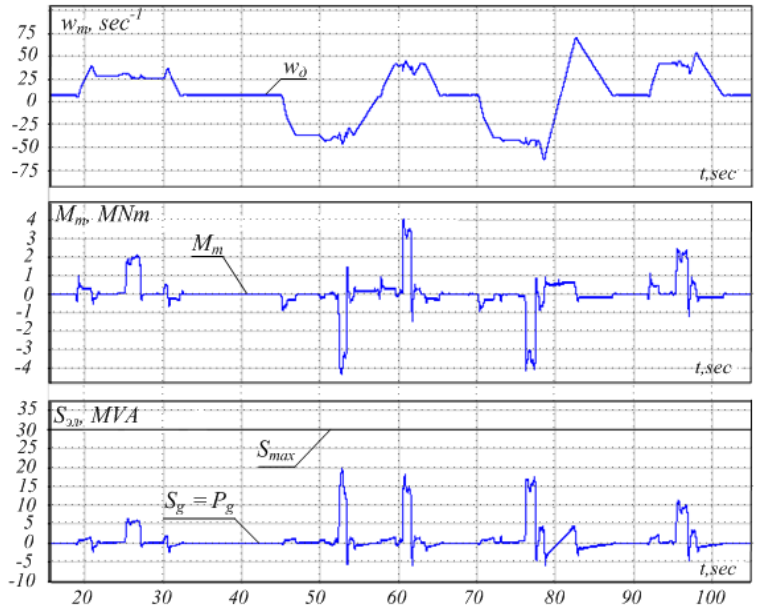

Figure 8. Operation condition at roughing

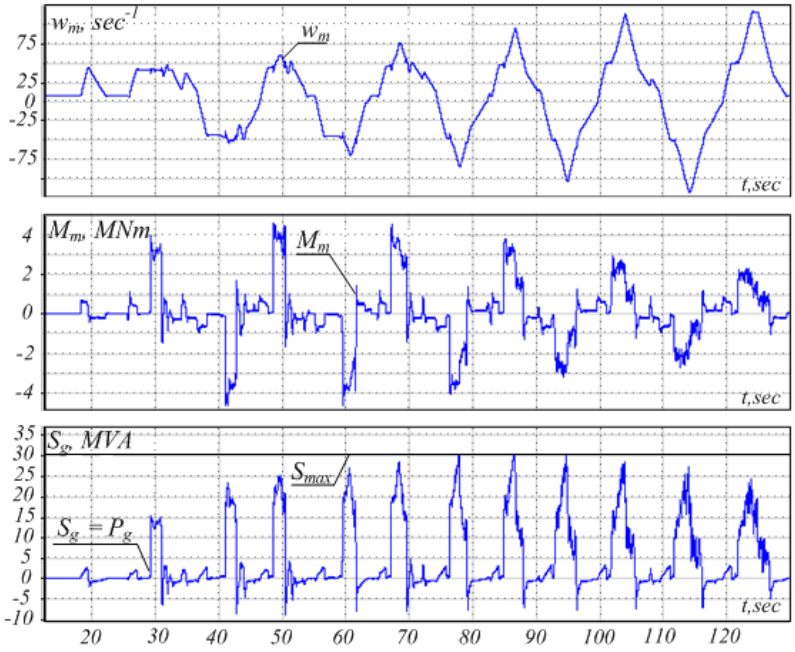

Figure 9. Operation condition at finish rolling

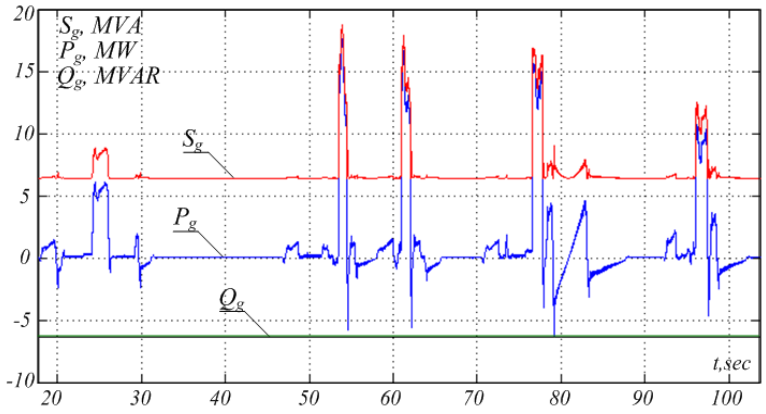

Figure 10. Reactive power generation at the roughing

6. CONCLUSION

The new reactive power compensation method in the industrial grid via high-power adjustable speed drives with the medium voltage 3L-NPC BtB converters has been proposed. It can be recommended to correct a power factor or compensate static or dynamic reactive power. A level of compensated reactive power should be calculated in accordance with load impedance diagrams and parameters of the grid side and 3L-NPC BtB converters.

An important advantage of the new method is that specialized equipment is not necessary for the implementation. The analysis of experimental research shows that the developed reactive power compensation method has been successfully applied for the main HP ASD of the plate mill rolling state 5000 (Magnitogorsk Iron and Steel Works, PJSC).

The huge prospects of HP ASDs with 3L-NPC BtB converters to integrate them into Smart Grid systems have been determined. It is a good solution as they are able to provide a high power flow and control a reactive power flow by the control system of 3L-NPC BtB converters. It can reduce a share of the consumed reactive power from the grid and improve power quality.

ACKNOWLEDGEMENTS

The work was supported by Act 211 Government of the Russian Federation, contract № 02.A03.21.0011.

REFERENCES

[1] J. Rodriguez, *et al.*, "Multilevel inverters: A survey of topologies, controls, and applications," *IEEE Trans. Ind. Electron.*, vol. 49, no. 4, pp. 724-738, 2002.
[2] A. K. Chattopadhyay, "Alternating current drives in the steel industry," *IEEE Ind. Electron. Mag.*, vol. 4, no. 4, pp. 30-42, 2010.
[3] H. Abu-Rub, *et al.*, Al-Haddad, *Power electronics for renewable energy systems, transportation and industrial applications*, New York: Wiley, 2014, p. 826.
[4] S. F. Seyed, "Investigation and comparison of multi-level converters for medium voltage applications," Dr.-Ing., Berlin, 2007
[5] B. Wu, *et al.*, *High-Power Converters and AC Drives*, 2nd Edition, New York: Wiley, 2017, p. 480.
[6] Frequency Converter Market by Type (Static and Rotary), by End-User (Aerospace & Defense, Power & Energy, Process Industry, Traction, Oil & Gas, and Marine/Offshore), and by Region - Global Forecast and Trends to 2020 [Online]. Available: http://www.marketsandmarkets.com/Market-Reports/frequency-converter-market-235193864.html
[7] HVDC Converter Station Market by Type (Monopolar, Bi-Polar, Back to Back, and Multi-Terminal), by Technology (Line Commutated Current Sourced Converters and Voltage Source Converters (VSC)), by Application and by Geography - Global Trends & Forecasts to 2019 [Online]. Available: http://www.marketsandmarkets.com/Market-Reports/hvdc-converterstation-market-243369221.html
[8] A. Siebert, *et al.*, "AC to dc power conversion now and in the future," *IEEE Trans. Ind. Appl.*, no. 38, pp. 934-940, 2002.
[9] J. Pontt, *et al.*, "Mitigation of noneliminated harmonics of SHEPWM three-level multipulse threephase active front end converter with low switching frequency for meeting standard IEEE-519-92," *IEEE Trans. Ind. Electron.*, vol. 19, no. 6, pp. 1594-1599, Nov., 2004.

[10] E. Pouresmaeil, *et al.*, "Multifunctional control of an NPC converter for the grid integration of renewable energy sources," in *Proc. 2015 IEEE Eindhoven PowerTech*, pp. 1-6.
[11] O. S. Senturk, *et al.*, "Medium voltage three-level converters for the grid connection of a multi-MW wind turbine," in. *Proc. 13th European Conference on Power Electronics and Applications, EPE '09*, Sept. 2009.
[12] R.-D. Klug, *et al.*, "High power medium voltage drives - innovations, portfolio, trends," in. *Proc. European Conference on Power Electronics and Applications*, Sept. 2005.
[13] A. Ojha, *et al.*, "Back to back connected multilevel converters: A review," *IOSR Journal of Electrical and Electronics Engineering (IOSR-JEEE)*, vol. 5, no. 5, pp. 57-57, 2013.
[14] S. Kouro, *et al.*, "Powering the future of industry: High-power adjustable speed drive topologies," *IEEE Ind. Appl. Mag.*, vol. 18, no. 4, pp. 26-39, 2012.
[15] B. Wu, *et al.*, *Power conversion and control of wind energy systems*, New York: Wiley, 2011, p. 456.
[16] M. Loonurm, *et al.*, "Tariffs for reactive power supplied from distribution networks," in. *Proc. Electric Power Quality and Supply Reliability Conf.*, June, 2010.
[17] J. Zhong, *et al.*, "Reactive power management in deregulated electricity markets-a review," in. *Proc. Power Engineering Society Winter Meeting IEEE*, Jan., 2002.
[18] J. Zhong, *et al.*, "Toward a competitive market for reactive power," *IEEE Trans. on Power Systems*, vol. 17, no. 4, pp. 1206-1215, 2002.
[19] H. Cai, *et al.*, "The comparison, study and proposal for China's reactive power pricing policy," in. *Proc. China International Conference on Electricity Distribution (CICED)*, Sept., 2012.
[20] C. Tufon, *et al.*, "A tariff for reactive power," in. *Proc. Power Systems Conference and Exposition, PSCE '09. IEEE/PES*, March, 2009.
[21] M. A. Golkar, *et al.*, "Reactive power pricing in deregulated electricity market," in. *Proc. 20th International Conference and Exhibition on Electricity Distribution - Part 1, CIRED*, June, 2009.
[22] A.S. Maklakov, *et al.*, "Power factor correction and minimization THD in industrial grid via reversible medium voltage AC drives based on 3L-NPC AFE rectifiers," in. *Proc. IECON Proceedings (Industrial Electronics Conference)*, pp. 2551-2556, 2016.
[23] X. Wang, *et al.*, "A review of power electronics based microgrids," *Journal of Power Electronics*, vol. 12, no. 1, pp. 181-192, 2012,
[24] T. R. Hramshin, *et al.*, "Evaluation of methods PWM voltage active rectifiers rolling mills," *Russian Internet Journal of Industrial Engineering*, no. 2, pp. 48-52, 2013.
[25] P. Pandit, *et al.*, "Real-time power quality measurements from a conventional AC dragline," *IEEE Trans. Ind. Appl.*, vol. 46, no. 5, pp. 1755-1763, 2010.
[26] R. Teodorescu, *et al.*, *Grid Converters for Photovoltaic and Wind Power Systems*, New York: Wiley, 2011, p. 416.
[27] A. Nabae, *et al.*, "A neutralpoint clamped PWM inverter," *IEEE Trans. Ind. Appl.*, vol. 1A-17, no. 5, pp. 518-523, 1981.
[28] N. Mohan, *et al.*, *Power Electronics book: Converters, Applications and Design*, New York: Wiley, 2003, p. 824.
[29] R. Melicio, *et al.*, "Comparative study of power converter topologies and control strategies for the harmonic performance of variable-speed wind turbine generator systems," *Energy*, vol. 36, pp. 520-529, 2011.
[30] A.S. Maklakov, *et al.*, "Integration prospects of electric drives based on back to back converters in industrial smart grid," in. *Proc. 12th International Conference on Actual Problems of Electronic Instrument Engineering*, pp. 770-774, 2014.
[31] A.A. Radionov, *et al.*, "Smart Grid for main electric drive of plate mill rolling stand," in. *Proc. International Conference on Mechanical Engineering, Automation and Control Systems*, 2015.
[32] A.A. Radionov, *et al.*, "New control method of back to back converter," in. *Proc. International Siberian Conference on Control and Communications*, 2015.

BIBLIOGRAPHY OF AUTHORS

1997 – Diploma of an engineer, Magnitogorsk State Technical University, Russia; 2000-PhD (technical science), Moscow State Technical University (MEI), Russia; 2009-Dr. Sc.(techn.), Magnitogorsk State Technical University, Russia; 2014 to present-Vice-Rector for Education Affairs, South Ural State University, Russia. His research interests include the field of power electronics, motor drive systems and mechatronics.

2007 – Diploma of an engineer, Magnitogorsk State Technical University, Russia; 2012-PhD (technical science), Magnitogorsk State Technical University, Russia; 2014 to present-Head of the Department "Mechatronics and automation", South Ural State University, Russia. His research interests include the field of mechatronics and motor drive systems.

2013 – Diploma of an engineer, Magnitogorsk State Technical University, Russia; 2017-PhD (technical science), South Ural State University, Russia; 2015 to present-Lecturer of the Department “Mechatronics and automation”, South Ural State University, Russia. His research interests include the field of power electronics and motor drive systems.

2015 – Diploma of an engineer, Magnitogorsk State Technical University, Russia; 2017-master's degree (technical science), South Ural State University, Russia; 2017 to present-Lecturer of the Department “Mechatronics and automation”, South Ural State University, Russia. Her research interests include the field of automation and control systems.